Earth and Planetary Science Letters 359–360 (2012) 240–247

Contents lists available at SciVerse ScienceDirect

Earth and Planetary Science Letters

journal homepage: www.elsevier.com/locate/epsl

How double volcanic chains sample geochemical anomalies from the lowermost mantle

Cinzia G. Farnetani [a,*], Albrecht W. Hofmann [b,c], Cornelia Class [b]

[a] Institut de Physique du Globe de Paris, Sorbonne Paris Cité, Univ Paris Diderot, UMR 7154, 75005 Paris, France
[b] Lamont Doherty Earth Observatory of Columbia University, Palisades, NY 10964, USA
[c] Max-Planck-Institut für Chemie, Postfach 3060, 55020 Mainz, Germany

ARTICLE INFO

Article history:
Received 22 May 2012
Received in revised form
19 September 2012
Accepted 27 September 2012
Editor: Y. Ricard
Available online 20 November 2012

Keywords:
mantle plumes
Hawaii
DUPAL
Pacific hotspots
isotopes

ABSTRACT

The distinct isotopic compositions of basalts from the two parallel tracks of Hawaiian volcanoes suggest a bilateral zonation of the underlying mantle plume, with an enriched southern side. Such zonation is not unique to Hawaii, but may well be a common feature of other Pacific hotspots. This remarkable isotopic pattern, revealed by double volcanic chains, appears to be related to the so-called DUPAL isotopic anomaly in the Pacific mantle, which correlates with the seismically imaged 'Large Low-Shear-Velocity Province'. Here we show how a large-scale isotopic gradient, exemplified by the radiogenic isotope ratio $^{208}Pb^*/^{206}Pb^*$, maps from the deep mantle into the Hawaiian plume conduit, and how it ultimately surfaces as $^{208}Pb^*/^{206}Pb^*$ variations in double-chain volcanoes. Our numerical simulations reveal a novel 'lobate' conduit structure which generates an overall bilateral isotopic zonation within the Hawaiian melting zone. Comparison between our model predictions and $^{208}Pb^*/^{206}Pb^*$ of several Hawaiian volcanoes shows that a deep-seated, north-south, isotopic gradient can explain the enriched southern (Loa) chain as well as the $^{208}Pb^*/^{206}Pb^*$ decline from shield to post-shield lavas, observed in several of the volcanoes. The results provide a mechanism for directly linking geochemical maps of ocean island basalts to the structure and composition of the lowermost mantle inferred by seismic tomography.

1. Introduction

What do plumes tell us about the distribution of geochemically distinct material in the Earth's mantle? This fundamental question seems far from being solved. Even for Hawaii, the best studied hotspot, two profoundly different models have been proposed to explain the distinct isotopic compositions between Kea and Loa-trend volcanoes. Models focused on a 'shallow origin' (Bianco et al., 2008; Ballmer et al., 2011) invoke differential melting of a mixture consisting of a relatively depleted peridotite and a fertile, geochemically enriched, eclogitic or pyroxenitic component. These components are assumed to be well stirred, so that the 'uniformly isotopically heterogeneous' plume lacks any compositional zonation. According to Ballmer et al. (2011) the topographic relief at the base of the oceanic lithosphere is responsible for differential melting between the northern (Kea) and the southern (Loa) side of the Hawaiian plume. In particular, a thinner lithosphere beneath the Kea-track volcanoes would induce higher melt fractions and preferential sampling of the isotopically depleted peridotite. However, this prediction is not confirmed by incompatible element abundances. For example, the La/Yb ratio, which is roughly inversely proportional to the melt fraction, is higher for Kea volcanoes, thereby indicating consistently lower melt fractions beneath the Kea-track (e.g., Hofmann ms. in prep.).

Models invoking a deep origin (Abouchami et al., 2005; Weis et al., 2011; Huang et al., 2011) relate the spatio-temporal geochemical variations of Hawaiian lavas to an internal zonation of the plume conduit, which ultimately reflects much larger-scale geochemical heterogeneities in the lowermost mantle. More specifically, the distinct lead isotopic compositions of Kea and Loa-trend volcanoes support a bilateral conduit structure (Abouchami et al., 2005) with an enriched Loa-side. According to Weis et al. (2011) the southern side of the Hawaiian plume preferentially samples isotopically enriched material from the edge of the 'Large Low-Shear-Velocity Province' (Romanowicz and Gung, 2002; Ritsema et al., 2011). Huang et al. (2011) provide a novel contribution to this debate by considering simultaneously three Pacific hotspots with double volcanic chains, namely Hawaii, Marquesas and Samoa. They find an interesting isotopic pattern: the volcanic chain located to the south (e.g., Loa-trend in Hawaii, Malu-trend in Samoa) has systematically higher

* Corresponding author.
E-mail addresses: cinzia@ipgp.fr, farnetani@ipgp.jussieu.fr (C.G. Farnetani), albrecht.hofmann@mpic.de (A.W. Hofmann), class@ldeo.columbia.edu (C. Class).

0012-821X/$ - see front matter © 2012 Elsevier B.V. All rights reserved.
http://dx.doi.org/10.1016/j.epsl.2012.09.057

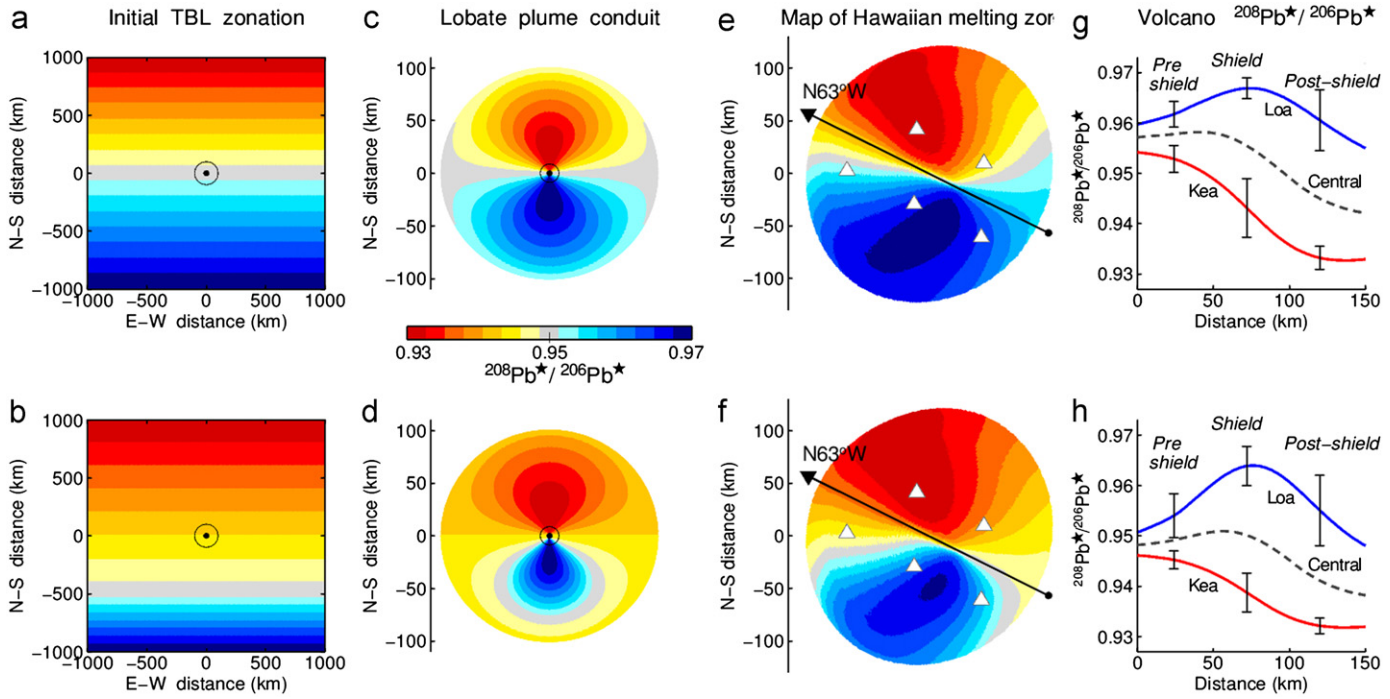

Fig. 1. (a) Map view of the thermal boundary layer (TBL). Initial condition. The dot indicates the plume conduit axis. Case A, with a constant and linear increase of $^{208}Pb^{\star}/^{206}Pb^{\star}$ from north to south. (b) Same as above, but for case B, where: (i) the conduit is displaced 500 km to the north of the mean $^{208}Pb^{\star}/^{206}Pb^{\star}$ value and (ii) the linear gradient is steeper in the southernmost 500 km. Note that, in both cases, the modeled $^{208}Pb^{\star}/^{206}Pb^{\star}$ ranges between 0.95 ± 0.02, and the mean $^{208}Pb^{\star}/^{206}Pb^{\star} = 0.95$ corresponds to Abouchami et al. (2005) dividing value between Loa- and Kea-trend volcanoes. We also assume that $^{208}Pb^{\star}/^{206}Pb^{\star}$ remains constant across the TBL height ($H_{TBL} = 100$ km). (c) Horizontal section of the lower mantle conduit after 60 Ma of plume lifetime. Case A. (d) Same as above, but for case B. (e) Calculated $^{208}Pb^{\star}/^{206}Pb^{\star}$ map of the Hawaiian melting zone for case A. We indicate the direction of the Pacific plate motion (arrow) and the schematic positions of Big Island volcanoes (triangles). (f) Same as above, but for case B. (g) Calculated $^{208}Pb^{\star}/^{206}Pb^{\star}$ evolution for an off-axis volcano belonging to the Loa- (blue line) and Kea-trends (red line) and for a centrally located volcano (dashed line). The standard deviation (vertical bars) indicates the $^{208}Pb^{\star}/^{206}Pb^{\star}$ variability within the magma capture zone. Horizontal axis: distance from the onset of melting calculated in the plate motion direction. Case A. (h) Same as above, but for case B.

$^{208}Pb/^{204}Pb$ at a given $^{206}Pb/^{204}Pb$ (thus higher $^{208}Pb^{\star}/^{206}Pb^{\star}$)[1] as well as higher $^{87}Sr/^{86}Sr$ and lower $^{143}Nd/^{144}Nd$ than the chain located to the north (e.g., Kea-trend in Hawaii, Vai-trend in Samoa). This shows that the Hawaiian-like geochemical structures may be a common feature of Pacific hotspots, best revealed by double volcanic chains.

Recently, Chauvel et al. (2012) have confirmed and further clarified the distinctive geochemical trends on the Marquesas. Somewhat similar geochemical zoning has been described for the Galápagos hotspot by Hoernle et al. (2000). Furthermore, the phenomenon is not restricted to Pacific hotspots, but similar, long-term isotopic 'tracks' also characterize the past 80 Ma-evolution of the Tristan-Gough hotspot track (Rohde et al., in press).

Another relevant observation is that $^{208}Pb^{\star}/^{206}Pb^{\star}$ increases from Hawaii to Samoa, thus suggesting a progressive involvement of deep material with a DUPAL fingerprint. It has long been known that the geochemical province known as 'DUPAL anomaly' (Dupré and Allègre, 1983; Hart, 1984) is correlated with the 'Large Low Shear Velocity Province' (LLSVP) in the lowermost mantle (Castillo, 1988; Wen, 2006). When this correlation is linked to the observation that many plumes rise from the edges of the Pacific LLSVP (Burke et al., 2008; Steinberger and Torsvik, 2012), and to the geochemical patterns observed on double volcanic chains (Weis et al., 2011; Huang et al., 2011), a strong case can be made that plumes not only rise from the deep mantle but also carry geochemical information from the deep.

Thus, recent geochemical studies support the idea that plumes carry messages from the lowermost mantle, but deciphering this message requires some fluid dynamics. So far, laboratory experiments (Kerr and Mériaux, 2004) and numerical simulations (Farnetani and Hofmann, 2009) have shown that geochemical zonation in the thermal boundary layer (TBL) at the base of the mantle may be 'preserved' in the plume conduit. However, these studies were limited to simple TBL zonations, either purely azimuthal or purely radial. No dynamical model has explored how a large-scale (DUPAL-like) isotopic gradient in the deep mantle maps into the plume conduit and ultimately affects the isotopic evolution of double volcanic chains. This is the objective of the present work. Our geochemical tracer is the isotope parameter $^{208}Pb^{\star}/^{206}Pb^{\star}$, also known as the 'radiogenic $^{208}Pb/^{206}Pb$ ratio', which is arguably the best geochemical discriminant between Loa-trend and Kea-trend volcanoes (Abouchami et al., 2005).

Here we consider the existence of a large-scale southward increase of $^{208}Pb^{\star}/^{206}Pb^{\star}$ in the lowermost mantle and address the following questions: (a) What is the resulting isotopic structure of the plume conduit? (b) What is the predicted $^{208}Pb^{\star}/^{206}Pb^{\star}$ zonation across the melting region of the Hawaiian plume? (c) If geographically distinct volcanoes are carried by the Pacific plate over such a zoned melting region, how does the isotopic signal evolve during the pre-shield, shield and post-shield volcanic stages? And, how do our model predictions compare with observations? Lastly, by varying the angle between the direction of the Pacific plate motion (N63°W) and the azimuth

[1] The lead isotope ratio $^{208}Pb^{\star}/^{206}Pb^{\star}$ reflects the ratio of $^{232}Th/^{238}U$ integrated over the Earth's history (Galer and O'Nions, 1985), and is defined as

$$^{208}Pb^{\star}/^{206}Pb^{\star} = \frac{(^{208}Pb/^{204}Pb)_{sample} - (^{208}Pb/^{204}Pb)_{primordial}}{(^{206}Pb/^{204}Pb)_{sample} - (^{206}Pb/^{204}Pb)_{primordial}}$$

where $(^{206}Pb/^{204}Pb)_{primordial} = 29.475$ and $(^{206}Pb/^{204}Pb)_{primordial} = 9.306$, based on Canyon Diablo Troilite.

of maximum $^{208}Pb^{*}/^{206}Pb^{*}$ gradient in the thermal boundary layer we explore under which conditions double volcanic chains are able to reveal deep geochemical zoning.

Parallel volcanic tracks appeared several times during the evolution of the Hawaiian-Emperor chain (Jackson and Shaw, 1975); the Kea–Loa tracks are the most recent of these. Double tracks may be caused by a change in tectonic-plate motion (Hieronymus and Bercovici, 1999, 2001) or/and by the arrival of fertile plume material that enhances melt productivity (Tanaka et al., 2008). It is beyond the scope of our paper to study the physical processes leading to the formation of parallel volcanic tracks, because this would require modeling the dynamic interaction between magma transport and lithospheric stresses.

2. The lobate conduit structure

To show how a large-scale geochemical gradient in the lowermost mantle maps into the plume conduit we use the numerical simulation by Farnetani and Hofmann (2009), which solves the conservation equations governing the plume-induced flow in the thermal boundary layer (TBL) and in the conduit. Deliberately, our model is purely thermal since it is instructive to consider the most basic fluid flow without the complexities of thermo-chemical plumes. We assume that $^{208}Pb^{*}/^{206}Pb^{*}$ increases linearly from north to south (N–S), thereby generating both azimuthal and radial variations. This southward gradient should be considered as an idealized, first-order approximation to a likely real $^{208}Pb^{*}/^{206}Pb^{*}$ distribution near the margin of the DUPAL belt. In case A (Fig. 1a) the geochemical gradient across the TBL is constant and the plume conduit is located directly above the mean $^{208}Pb^{*}/^{206}Pb^{*}$ value, whereas in case B (Fig. 1b) the conduit is displaced by 500 km toward the north of the mean $^{208}Pb^{*}/^{206}Pb^{*}$. The resulting conduit structure features a novel 'lobate' geochemical zonation (Fig. 1c and d): the $^{208}Pb^{*}/^{206}Pb^{*}$ distribution is globally bilateral, yet, there are considerable azimuthal and radial variations due to the formation of two internally zoned lobes. The highest $^{208}Pb^{*}/^{206}Pb^{*}$ variability occurs in the N–S direction, as expected, but the most extreme $^{208}Pb^{*}/^{206}Pb^{*}$ values are now close to the axis (radial distance $r < 50$ km), whereas in the TBL they were at $r_{TBL} \sim 1000$ km, as explained in the next paragraph. In case B the conduit structure is still bilateral, although not symmetric (Fig. 1d), thereby showing that, independently of the specific zonation in the TBL, a large-scale $^{208}Pb^{*}/^{206}Pb^{*}$ gradient generates a 'lobate' and overall bilateral conduit structure. Note that our results can be extended to any direction of maximum isotopic gradient by a trivial rotation of both TBL and conduit maps.

To help visualize the development of the 'lobate' structure, Fig. 2 shows the flow of two geochemically distinct bands whose initial positions are 200–300 km north and 500–600 km south of the conduit axis, respectively. While flowing to the plume stem, each band acquires a fan shape with a clear cusp in the N–S direction (Fig. 2a). Material in the TBL undergoes simple shear, since the radial velocity V_r increases with depth towards the hot, low-viscosity, base of the TBL. Within the TBL pure shear becomes important only close to the plume axis. The conduit cross section at $H = 500$ km (inset of Fig. 2b) shows that the orange band first appears on the north side and close to the axis. Over time (Fig. 2c), the lobe extends to greater r and larger azimuths, reflecting, respectively, the arrivals from shallower TBL depths and from increasing angular aperture. In three dimensions, the 'lobe' has a tube-like structure: its inner part is actually filled by material coming from increasingly distant zones of the TBL. This explains why the most extreme $^{208}Pb^{*}/^{206}Pb^{*}$ values (i.e., at initial $r_{TBL} \sim 1000$ km) end up close to the conduit axis. Finally, we note that the 'lobate' geochemical zonation forms regardless of the initial distance of the band, as long as the plume is sufficiently long-lived.

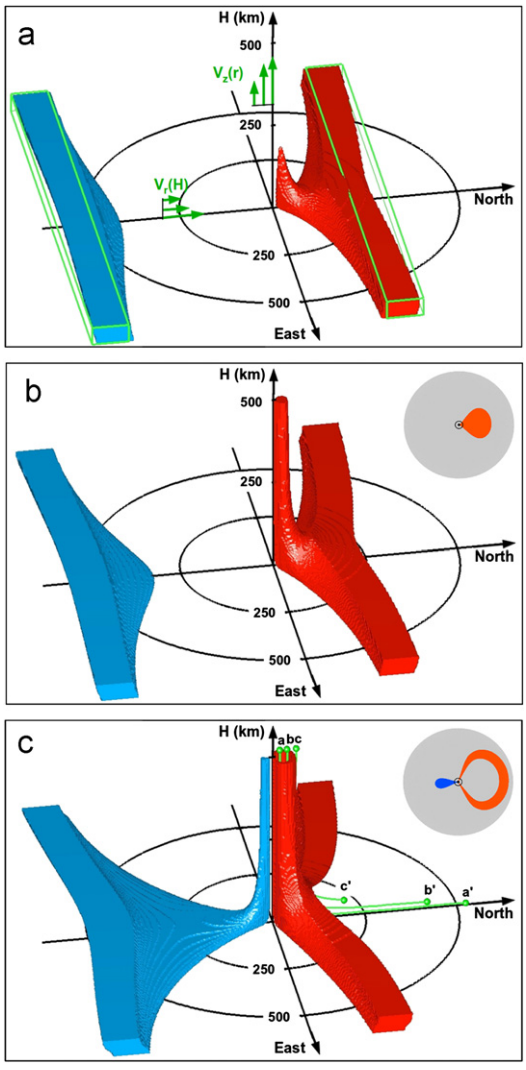

Fig. 2. Part of the modeled thermal boundary layer (TBL). (a) Green lines: initial position of two geochemically distinct bands, 200–300 km north and 500–600 km south of the plume axis. In orange and blue: position and shape of the two bands after 2.5 Ma from the initial condition. Green arrows: Schematic representation of the velocity field, the radial V_r and vertical V_z components are functions of height H and radial distance r, respectively. The flow is axisymmetric and radially converges to the plume stem. (b) Position and shape of the two bands after 4.5 Ma. Inset: cross section of the plume conduit at $H = 500$ km. Conduit material that does not belong to the selected bands is shown in grey. (c) Position and shape of the two bands after 11 Ma. The 'hollow tube' appearance occurs because we do not represent TBL material further to the North, which would fill the inner part of the lobe. Particle trajectories a–a′, b–b′, c–c′ (green) show that material side by side in the conduit actually comes from distinct zones of the TBL because: $r_{a'} > r_{b'} > r_{c'}$ and $H_{a'} < H_{b'} < H_{c'}$. (For interpretation of the references to color in this figure caption, the reader is referred to the web version of this article.)

3. $^{208}Pb^{*}/^{206}Pb^{*}$ of Hawaiian volcanoes: model predictions and observations

How does the 'lobate' structure of the conduit map into the melting zone of the Hawaiian plume? To answer this question, we use a numerical simulation of a vigorous plume sheared by a fast moving (9×10^{-2} m/yr) Pacific plate (Farnetani and Hofmann, 2010). We calculate the trajectories of more than a million passive tracers, with each tracer carrying a $^{208}Pb^{*}/^{206}Pb^{*}$ value according

to its position in the conduit (Fig. 3). The $^{208}Pb^{*}/^{206}Pb^{*}$ distribution inside the three-dimensional melting zone is then converted to a $^{208}Pb^{*}/^{206}Pb^{*}$ map by vertically integrating over the entire melting column. Note that we neglect melt transport processes, which are unlikely to affect isotope ratios. For case A the map (Fig. 1e) shows a large-scale $^{208}Pb^{*}/^{206}Pb^{*}$ bilateral zonation, with higher values on the southern side of the melting region. On a smaller scale, the complex $^{208}Pb^{*}/^{206}Pb^{*}$ distribution is due to the combined effect of plume material flowing in the plate motion direction and spreading laterally beneath the lithosphere. A similar large-scale bilateral zonation is found for case B (Fig. 1f), but the zone with high $^{208}Pb^{*}/^{206}Pb^{*}$ is narrower.

To predict the temporal isotopic evolution of a given volcano, we calculate the average $^{208}Pb^{*}/^{206}Pb^{*}$ within a 'magma capture zone' (MCZ) of 30 km radius, from where, ideally, melts rise to the overlying volcanic edifice. Figs. 1g and 1h show that, for both cases, a Loa-trend volcano has consistently higher $^{208}Pb^{*}/^{206}Pb^{*}$ than a Kea-trend one. Moreover, the temporal $^{208}Pb^{*}/^{206}Pb^{*}$ evolution of the two trends is different: for a Loa-trend volcano, shield-stage lavas have higher $^{208}Pb^{*}/^{206}Pb^{*}$ than pre- and post-shield lavas, whereas, for a Kea-trend volcano $^{208}Pb^{*}/^{206}Pb^{*}$ progressively decreases from pre- to post-shield stages. Comparison with the evolution of a central volcano shows the importance of double volcanic chains for revealing the bilateral zonation within the plume.

We now test the above predictions by plotting $^{208}Pb^{*}/^{206}Pb^{*}$ ratios for all six Big Island volcanoes (Fig. 4) from the GEOROC database (find complete references in the figure caption). Distances in the direction of plate motion are approximated schematically from geologic data indicating pre-shield, shield, late-shield, and post-shield phases. For Loa-trend volcanoes, the following observations agree with our predictions: (a) Shield lavas from the submarine flanks of Mauna-Loa, spanning a depth range 2290–489 mbsl (Weis et al., 2011) have the highest $^{208}Pb^{*}/^{206}Pb^{*}$. (b) Late-shield, mainly subaerial, Mauna-Loa lavas have lower $^{208}Pb^{*}/^{206}Pb^{*}$ values, (c) Hualalai post-shield lavas (Hanano et al., 2010) have even lower $^{208}Pb^{*}/^{206}Pb^{*}$, not only with respect to Mauna-Loa but also with respect to Hualalai shield-stage (Yamasaki et al., 2009). For Kea volcanoes the model predicts decreasing values from shield to post-shield stages, similar to the observed evolution of Mauna Kea lavas from shield (Eisele et al., 2003; Blichert-Toft and Albarède, 2009) to post-shield (Hanano et al., 2010; Abouchami et al., 2005) and the evolution of Kohala lavas from late-shield to post-shield (Hanano et al., 2010; Abouchami et al., 2005).

It is clear that there is rather large scatter in the observed $^{208}Pb^{*}/^{206}Pb^{*}$ ratios. One difficulty is that the actual long-term temporal evolution of all of these volcanoes, except Mauna Kea, is

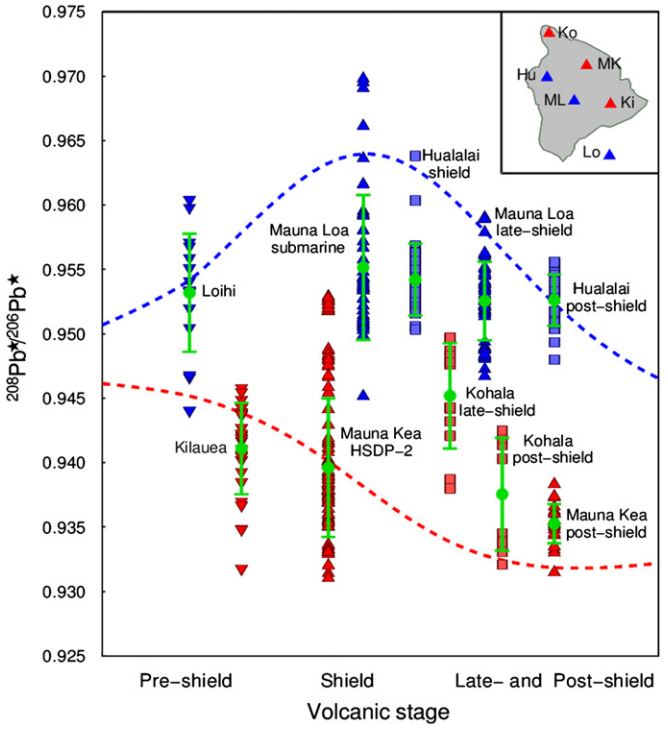

Fig. 4. $^{208}Pb^{*}/^{206}Pb^{*}$ for Loa (blue symbols) and Kea-trend (red symbols) Big Island volcanoes. In green: the standard deviation and the mean (circle). Dashed lines: model predictions for case B (as in Fig. 1h). Note that the position on the horizontal axis is schematically ordered in the sequence: pre-shield, early-shield, shield, late-shield, and post-shield. Inset: map of Big Island volcanoes. References to data used: For Loihi, Abouchami et al. (2005) and Ren et al. (2009). For Mauna Loa submarine, data by Weis et al. (2011) from 'Jason 2 Mile High basalts' and from 'Pisces Dives-Dredging'. For Mauna Loa late-shield, HSDP data by Abouchami et al. (2000); historic and pre-historic lavas by Weis et al. (2011). For Hualalai shield, Yamasaki et al. (2009). For Hualalai post-shield, Hanano et al. (2010). For Kilauea, Abouchami et al. (2005) and Tanaka and Nakamura (2005). For Mauna Kea, HSDP-2, Eisele et al. (2003) and Blichert-Toft and Albarède (2009). For Mauna Kea, post-shield, Hanano et al. (2010) and Abouchami et al. (2005). For Kohala, late-shield, Hanano et al. (2010) and 'W-samples' by Abouchami et al. (2005). For Kohala, post-shield, Hanano et al. (2010) and 'M-samples' by Abouchami et al. (2005). (For interpretation of the references to color in this figure caption, the reader is referred to the web version of this article.)

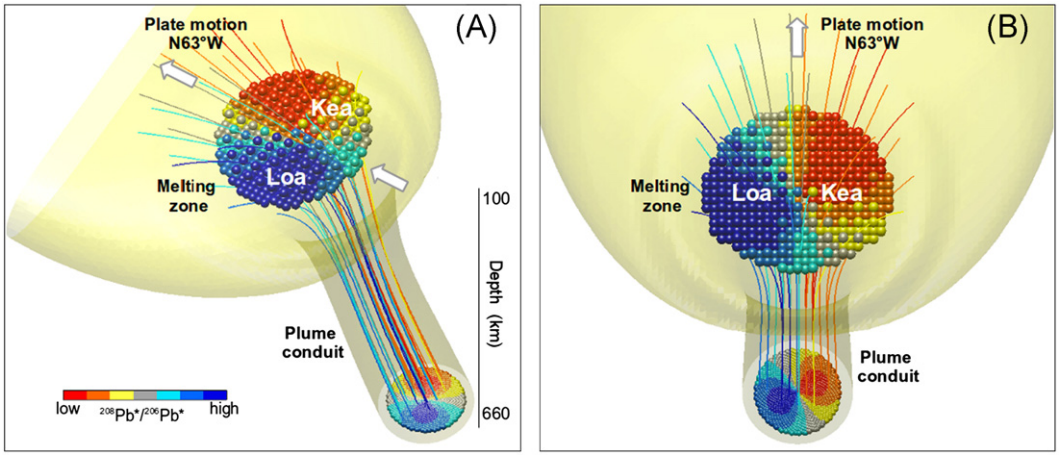

Fig. 3. Numerical simulation of the Hawaiian plume calculated using Tackley (1998) Stag3D code. Surface at constant temperature (yellow) in the upper mantle. $^{208}Pb^{*}/^{206}Pb^{*}$ zonation across the conduit and the melting zone (colored dots), flow trajectories (colored lines) for case A. (A) Side view. (B) Top view. (For interpretation of the references to color in this figure caption, the reader is referred to the web version of this article.)

known only approximately. To check whether the mean values given on Fig. 4 show statistically significant declines from shield to post-shield phases at the 95% confidence limit, we calculate standard errors of the mean multiplied by a factor appropriate for the specific number of samples in each set (this multiplier is 1.96 for an infinite number of samples and 2.09 for 20 samples, for example). For Mauna Loa, we obtain a significant decrease of $^{208}Pb^{*}/^{206}Pb^{*}$ from 0.95516 ± 0.00017 ($n=42$) for the submarine lava average to 0.95296 ± 0.00078 ($n=59$) for the late-shield average. For Kohala, the mean value decreases significantly from 0.9428 ± 0.0028 ($n=11$, shield average) to 0.9346 ± 0.0027 ($n=9$, post-shield average). The exception is Hualalai, where the decrease from 0.9542 ± 0.0010 ($n=31$) to 0.9534 ± 0.0010 ($n=13$) is not statistically significant.

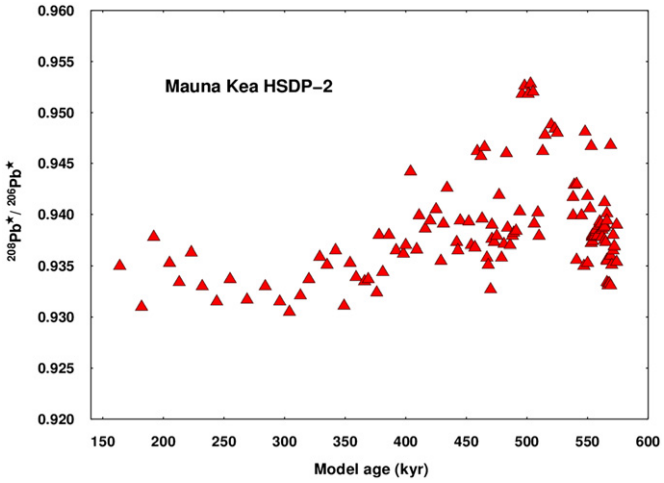

Fig. 5. Model age vs. $^{208}Pb^{*}/^{206}Pb^{*}$ for Mauna Kea samples (Eisele et al., 2003; Blichert-Toft and Albarède, 2009) from the Hawaiian Scientific Drilling Project (HSDP-2). Stratigraphic depth is recalculated in terms of model ages according to the growth model by DePaolo and Stolper (1996).

The only volcano for which we have a detailed long-term record of eruptions is Mauna Kea, because sampling from the Hawaiian Scientific Drilling Project (HSDP-2) enables a more adequate assessment of the isotopic evolution over the last 600 kyr. In spite of the rather large scatter of data, the HSDP-2 record shows a clear decline of $^{208}Pb^{*}/^{206}Pb^{*}$ (Fig. 5), consistent with our model predictions. A simple linear correlation through these 131 samples yields a correlation coefficient of 0.36, which is significant at the 0.999 confidence level.

The overall agreement between observed and predicted $^{208}Pb^{*}/^{206}Pb^{*}$ for all Big Island volcanoes shows that our model can provide a fluid dynamically consistent framework to interpret isotope trends on length scales of several tens of kilometers and time scales of 300 kyr and greater. Our model, however, does not address rapid geochemical fluctuations. Note that smaller-scale geochemical variations may be superimposed on the large-scale trends. For example, small-scale (on the order of 10–100 km) heterogeneities scattered in the TBL may coexist with the modeled large-scale (order 10^3 km) southward $^{208}Pb^{*}/^{206}Pb^{*}$ increase. Such heterogeneities, stretched by the plume flow into geochemically distinct filaments (Farnetani and Hofmann, 2010) would generate, upon melting, an additional $^{208}Pb^{*}/^{206}Pb^{*}$ spatial variability with respect to the trends shown in Fig. 4.

Data for older Hawaiian volcanoes are less abundant and we consider only four volcanoes for which high-quality Pb-isotope data exist and record the evolution from shield to post-shield phases. This is not the case, for example, for Lanai or Kahoolawe, which are therefore not included here. For Haleakala (Fig. 6a) and West Maui (Fig. 6b) both Kea-trend volcanoes, $^{208}Pb^{*}/^{206}Pb^{*}$ decreases from shield to post-shield phases, in agreement with model prediction. West Molokai, a Loa-trend volcano, also shows a decreasing trend from shield to post-shield (Fig. 6c), although $^{208}Pb^{*}/^{206}Pb^{*}$ varies over a much wider range with respect to our model.

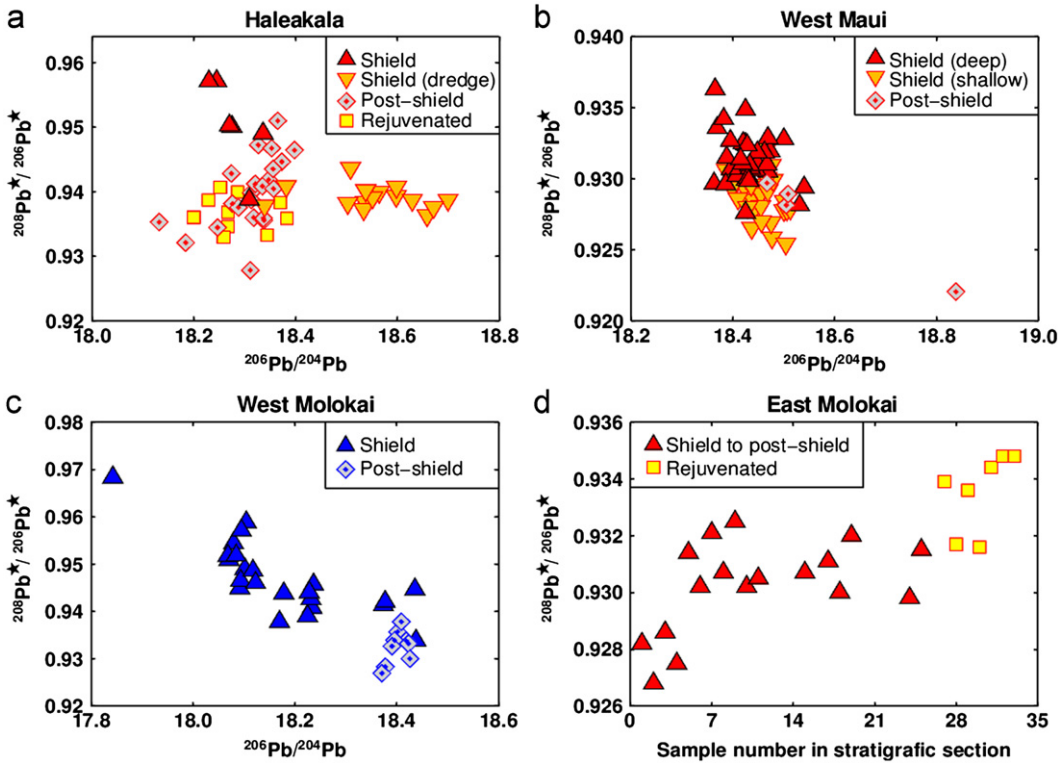

Fig. 6. $^{206}Pb/^{204}Pb$ vs. $^{208}Pb^{*}/^{206}Pb^{*}$ for: (a) Haleakala, Chen et al. (1991), Ren et al. (2006), West and Leeman (1987). (b) West Maui, Gaffney et al. (2004). (c) West-Molokai, Xu et al. (2007). (d) Sample number across stratigraphic sequence vs. $^{208}Pb^{*}/^{206}Pb^{*}$ for East-Molokai, Xu et al. (2005).

East Molokai, a Kea-trend volcano, is an apparent exception to these generally decreasing $^{208}Pb^{\star}/^{206}Pb^{\star}$ trends, because $^{208}Pb^{\star}/^{206}Pb^{\star}$ values increase from late-shield to post-shield and rejuvenated phases (Fig. 6d). Nevertheless, an increasing $^{208}Pb^{\star}/^{206}Pb^{\star}$ during the late-stage of aKea-side volcano is consistent with our model predictions (see below) if one takes into account a change in absolute plate motion. As discussed by Abouchami et al. (2005), near the Molokai fracture zone, there is a bend in the azimuth of the hotspot trace, indicating a change in absolute plate motion (Wessel and Kroenke, 1997). Three million years ago the Pacific plate direction was more westerly, so that $\phi_{3Ma} > 63^{\circ}$, where ϕ is the angle between the plate motion direction and the direction of maximum geochemical gradient in the TBL.

4. Changing ϕ, the angle between plate direction and the direction of isotopic gradient in the TBL

Up to now we have considered a constant plate motion direction (N63°W) and a constant N–S direction of maximum geochemical gradient in the TBL, so that $\phi = 63^{\circ}$. However, it is appropriate to calculate the effect of varying ϕ, in order to address a different plate motion direction in the past, and to test how our results depend on the assumed N–S gradient. Fig. 7 shows that for $\phi = 90^{\circ}$ (Fig. 7a) the $^{208}Pb^{\star}/^{206}Pb^{\star}$ distribution across the melting zone is bilaterally symmetrical (Fig. 7b). Therefore, parallel volcanic chains have distinct and opposite $^{208}Pb^{\star}/^{206}Pb^{\star}$ evolution (Fig. 7c), whereas a central volcano, which samples the two sides equally, has constant $^{208}Pb^{\star}/^{206}Pb^{\star}$. Notably, for a Kea-trend volcano we predict that $^{208}Pb^{\star}/^{206}Pb^{\star}$ increases during the post-shield stage, in agreement with the evolution of East Molokai lavas. (Note that in Fig. 7 we show changes in the direction of the gradient, leaving the direction of plate motion constant. The case of East Molokai is equivalent, because the approximate angle of $\phi = 90^{\circ}$ is produced by changing the direction of plate motion and leaving the isotopic gradient in the N–S direction). For $\phi = 45^{\circ}$ (Fig. 7d), the $^{208}Pb^{\star}/^{206}Pb^{\star}$ distribution across the melting zone is overall bilateral (Fig. 7e) and the predicted geochemical evolution of Loa and Kea-trend volcanoes is similar but with higher $^{208}Pb^{\star}/^{206}Pb^{\star}$ for the Loa-side (Fig. 7f). Finally, for $\phi = 0^{\circ}$ (Fig. 7g), when the direction of maximum geochemical gradient in the TBL is identical to the direction of the plate motion, a completely novel geochemical zonation appears (Fig. 7h), reminiscent of the horse-shoe pattern

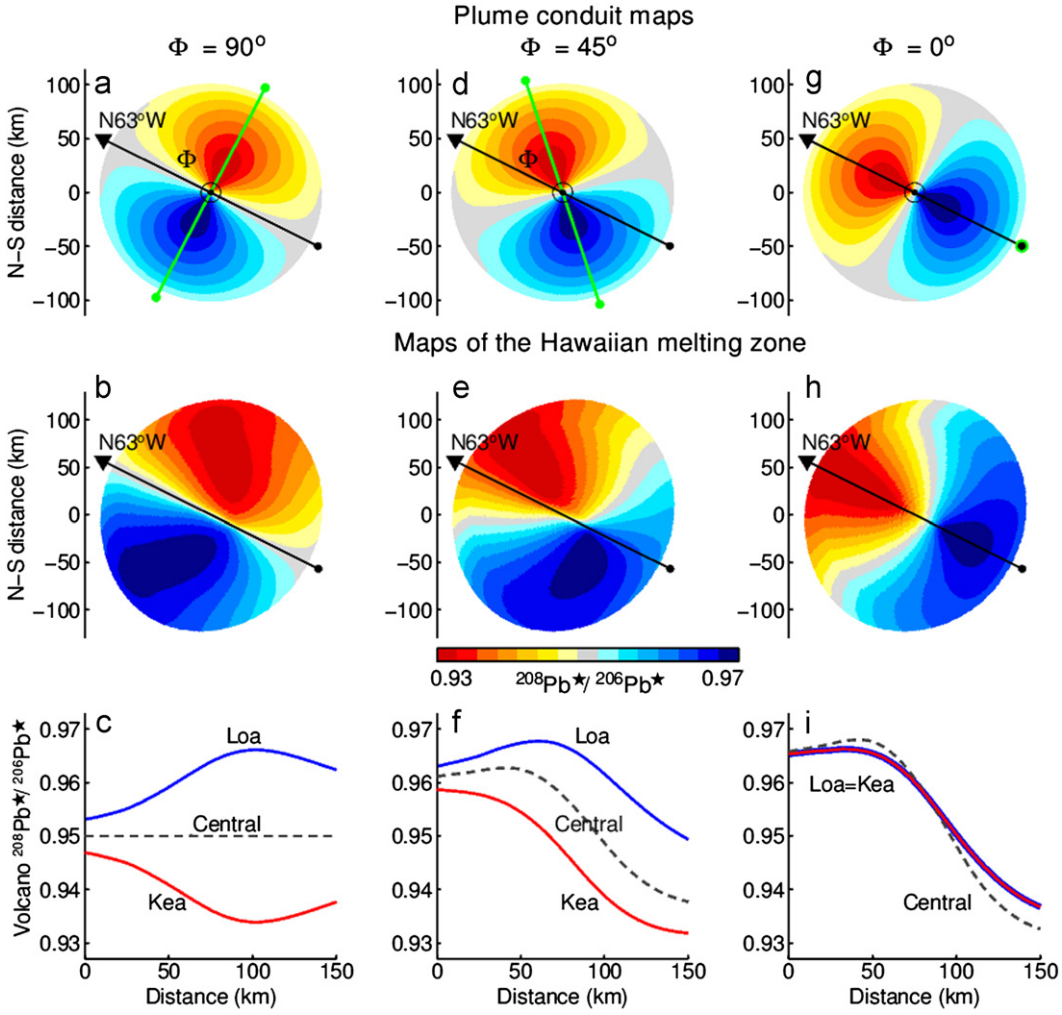

Fig. 7. Effect on conduit structure of different angles ϕ between the direction plate motion (black arrows) and the direction of maximum isotopic gradient in the thermal boundary layer (green bar). Similarly to the initial condition of case A, the conduit is placed above the mean $^{208}Pb^{\star}/^{206}Pb^{\star}$ and the isotopic gradient is constant. Top: plume conduit structure. Middle: predicted geochemical zonation across the Hawaiian melting zone. Bottom: predicted geochemical variability for a central volcano (dashed line), for a Loa- (blue line) and Kea-trend (red line) volcano. (a–c) For $\phi = 90^{\circ}$. (d–f) For $\phi = 45^{\circ}$. (g–i) For $\phi = 0^{\circ}$. (For interpretation of the references to color in this figure caption, the reader is referred to the web version of this article.)

observed for the Galápagos archipelago (Harpp and White, 2001; Hoernle et al., 2000). Only in such a case will two parallel volcanic chains be geochemically identical (Fig. 7i).

This figure shows that the bilateral zonation of the Hawaiian plume can be obtained for a range of ϕ (i.e., $45^\circ < \phi < 90^\circ$), therefore our results for $\phi = 63^\circ$ do not depend severely on the assumed north-south direction of the geochemical gradient.

We also note that for hotspots on the southern side of the DUPAL belt, the direction of isotopic enrichment should be flipped by 180°, so that the northern volcanic chain becomes be the enriched one, as observed at the Societies hotspot (Payne et al., in press). Fig. 7 provides model predictions that could be tested for other hotspots, such as Galápagos on the Nazca plate or Tristan-Gough in the South Atlantic, but this is beyond the scope of the present paper.

5. Continuity of the Hawaiian conduit across the transition zone

In this work we have assumed a continuous plume conduit across the mantle, so that its geochemical zonation is not significantly perturbed by the transition zone. However, thermo-chemical plumes may spread at the base of the phase transition (Farnetani and Samuel, 2005) and purely thermal plumes may acquire, under specific conditions, a particular morphology beneath the 660 km discontinuity (Tosi and Yuen, 2011). It is thus crucial to seismically image the Hawaiian plume across and below the transition zone.

In a zone southeast of Hawaii, SS-wave precursor studies (Schmerr and Garnero, 2006; Schmerr et al., 2010) found a thinned transition zone, furthermore, S-wave (Wolfe et al., 2009) and P-wave (Wolfe et al., 2011) tomography imaged a low-velocity anomaly that extends from the upper into the lower mantle. These studies independently support the presence of a continuous Hawaiian conduit, slightly tilted in the plate motion direction, as previously argued by Steinberger et al. (2004).

Using inverse scattering of SS waves, Cao et al. (2011) detected a thinned transition zone to the southeast of Hawaii. However, contrary to previous interpretations, these authors locate the source of the Hawaiian plume 1000–1500 km to the west of the hotspot. In this zone ($\sim 15^\circ$ longitude west of Hawaii) Cao et al. (2011) find a depression of the 660 km discontinuity, which they call '*enigmatic*', but then interpret as hot, ponded material, undergoing the post-garnet transition. There are two limitations to their model: First, the transition from majorite-garnet to an Al-bearing Mg-rich Perovskite has a positive Clapeyron slope (Hirose, 2002; Yu et al., 2011) and therefore does not act as a barrier to the upwelling flow. Clearly, more work is needed to elucidate the dynamics of a hot plume undergoing an exothermic and an endothermic phase transition roughly at the same depth. Second, Cao et al. (2011) neither image, nor propose, any physical connection between the active Hawaiian volcanism and the distant ponded material. We therefore regard their conclusion that "*zonation of mantle plumes must be shallow-mantle phenomena*" to be premature, and we favor models with a continuous plume conduit to the southeast.

6. Conclusion

Using numerical simulations of a vigorous thermal plume, we have shown that:

1. A large-scale southward increase of $^{208}Pb^*/^{206}Pb^*$ in the lowermost mantle generates a new zonation in the plume conduit, which we call 'lobate'. The structure is overall bilateral, but shows surprising complexities induced by the flow. The 'lobate' structure has never been described before, because all previous models were limited to purely azimuthal or purely radial variations across the TBL. Instead, latitudinal variations across the TBL generate simultaneously azimuthal *and* radial variations so that the resulting conduit structure is 'lobate'.
2. The calculated $^{208}Pb^*/^{206}Pb^*$ zonation of the Hawaiian melting zone is globally bilateral, thereby explaining the distinct $^{208}Pb^*/^{206}Pb^*$ between Loa and Kea-trend volcanoes. We also predict the long time-scale (e.g., 300 kyr) $^{208}Pb^*/^{206}Pb^*$ evolution of Kea and Loa-side volcanoes. We find that the predicted $^{208}Pb^*/^{206}Pb^*$ decrease from shield to post-shield stages fits reasonably well available observations for all Big Island volcanoes, and for older volcanoes for which high-quality Pb-isotope data exist.
3. Double volcanic chains provide a unique opportunity to reveal the bilateral nature of a plume, in particular when the angle ϕ (i.e., the angle between the plate motion direction and the direction of maximum geochemical gradient in the TBL) is greater than 45°. We argue that geochemically distinct double volcanic chains should be the rule, rather than the exception, whenever large-scale geochemical gradients exist in the lower mantle.

Both Castillo (1988) and Wen (2006) have pointed out the connection between the DUPAL anomaly and the seismically detected 'Large Low Shear Velocity Province' in the Central Pacific. Although we have only modeled the $^{208}Pb^*/^{206}Pb^*$ fingerprint of the DUPAL anomaly, the satisfactory agreement between model predictions and geochemical observations for numerous Hawaiian volcanoes, lends indirect, but strong support to the idea that plumes rise from the edges (Burke et al., 2008; Steinberger and Torsvik, 2012) of 'Large Low Shear Velocity Province' and that this can be traced by the geochemical 'smoke signals' brought to the surface by mantle plumes.

Acknowledgments

We thank Janne Blichert-Toft and an anonymous reviewer for their insightful and constructive reviews. We also thank Dominique Weis and Francis Albarède for discussions and Yanick Ricard for his editorial handling. This work has been supported by ANR-10-BLANC-0603 program funded by the French Agence National de la Recherche. IPGP Contribution No. 3336; LDEO Contribution No. 7612.

References

Abouchami, W., Galer, S.J.G., Hofmann, A.W., 2000. High precision lead isotope systematics of lavas from the Hawaiian Scientific Drilling Project. Chem. Geol. 169, 187–209.

Abouchami, W., Hofmann, A.W., Galer, S.J.G., Frey, F., Eisele, J., Feigenson, M., 2005. Pb isotopes reveal bilateral asymmetry and vertical continuity in the Hawaiian plume. Nature 434, 851–856.

Ballmer, M.D., Ito, G., van Hunen, J., Tackley, P.J., 2011. Spatial and temporal variability in Hawaiian hotspot volcanism induced by small-scale convection. Nat. Geosci. 4, 457–460, http://dx.doi.org/10.1038/NGEO1187.

Bianco, T.A., Ito, G., van Hunen, J., Ballmer, M.D., Mahoney, J.J., 2008. Geochemical variation at the Hawaiian hot spot caused by upper mantle dynamics and melting of a heterogeneous plume. Geochem. Geophys. Geosyst. 9, http://dxdoi.org/10.1029/2008GC002111.

Blichert-Toft, J., Albarède, F., 2009. Mixing and isotopic heterogeneities in the Mauna Kea plume conduit. Earth Planet. Sci. Lett. 282, 190–200.

Burke, K., Steinberger, B., Torsvik, T.H., Smethurst, M.A., 2008. Plume generation zones at the margins of large low shear velocity provinces on the core-mantle boundary. Earth Planet. Sci. Lett. 265, 49–60.

Cao, Q., van der Hilst, R.D., de Hoop, M.V., Shim, S.-H., 2011. Seismic imaging of transition zone discontinuities suggests hot mantle west of Hawaii. Science 332, 1068–1071.

Castillo, P., 1988. The Dupal Anomaly as a trace of the upwelling lower mantle. Nature 336, 667–670.

Chauvel, C., Maury, R.C., Blais, S., Lewin, E., et al., 2012. The size of plume heterogeneities constrained by Marquesas isotopic stripes. Geochem. Geophys. Geosyst. 13, http://dxdoi.org/10.1029/2012GC004123.

Chen, C.Y., et al., 1991. The tholeiite to alkalic basalt transition at Haleakala Volcano, Maui, Hawaii. Contrib. Mineral. Petrol. 106, 183–200.
DePaolo, D.J., Stolper, E.M., 1996. Models of Hawaiian volcano growth and plume structure: implications of results from the Hawaii scientific drilling project. J. Geophys. Res. 101, 11643–11654.
Dupré, B., Allègre, C.J., 1983. Pb–Sr isotope variation in Indian Ocean basalts and mixing phenomena. Nature 303, 142–146.
Eisele, J., Abouchami, W., Galer, S.J.G., Hofmann, A.W., 2003. The 320 kyr Pb isotope evolution of the Mauna Kea lavas recorded in the HSDP-2 drill core. Geochem. Geophys. Geosyst. 4, http://dxdoi.org/10.1029/2002GC000339.
Farnetani, C.G., Samuel, H., 2005. Beyond the thermal plume paradigm. Geophys. Res. Lett. 32, http://dxdoi.org/10.1029/2005GL022360.
Farnetani, C.G., Hofmann, A.W., 2009. Dynamics and internal structure of a lower mantle plume conduit. Earth Planet. Sci. Lett. 282, 314–322.
Farnetani, C.G., Hofmann, A.W., 2010. Dynamics and internal structure of the Hawaiian plume. Earth Planet. Sci. Lett. 295, 231–240.
Gaffney, A.M., Nelson, B.K., Blichert-Toft, J., 2004. Geochemical constraints on the role of oceanic lithosphere in intra-volcano heterogeneity at West Maui, Hawaii. J. Petrol. 45, 1663–1687.
Galer, S.J.G., O'Nions, R.K., 1985. Residence time of thorium uranium, and lead in the mantle with implications for mantle convection. Nature 316, 778–782.
Hanano, D., Weis, D., Scoates, J.S., Aciego, S., DePaolo, D.J., 2010. Horizontal and vertical zoning of heterogeneities in the Hawaiian mantle plume from the geochemistry of consecutive postshield volcano pairs: Kohala-Mahukona and Mauna Kea-Hualalai. Geochem. Geophys. Geosyst. 11, http://dxdoi.org/10.1029/2009GC002782.
Harpp, K.S., White, W.M., 2001. Tracing a mantle plume: isotopic and trace element variations of Galápagos seamounts. Geochem. Geophys. Geosyst. 2, http://dx.doi.org/10.1029/2000GC000137.
Hart, S.R., 1984. A large-scale isotope anomaly in the Southern Hemisphere mantle. Nature 309, 753–757.
Hieronymus, C.F., Bercovici, D., 1999. Discrete, alternating hotspot islands formed by the interaction of magma transport and lithospheric flexure. Nature 397, 604–607.
Hieronymus, C.F., Bercovici, D., 2001. A theoretical model of hotspot volcanism: control on volcanic spacing and patterns via magma dynamics and lithospheric stresses. J. Geophys. Res. 106, 683–702, http://dx.doi.org/10.1029/2000JB900355.
Hirose, K., 2002. Phase transitions in pyrolitic mantle around 670-km depth: implications for upwelling of plumes from the lower mantle. J. Geophys. Res. 107, http://dx.doi.org/10.1029/2001JB000597.
Hoernle, K., Werner, R., Phipps Morgan, J., Garbe-Schonberg, D., Bryce, J., Mrazek, J., 2000. Existence of complex spatial zonation in the Galápagos plume for at least 14 m y. Geology 28, 435–438.
Huang, S., Hall, P.S., Jackson, M.G., 2011. Geochemical zoning of volcanic chains associated with Pacific hotspots. Nat. Geosci. 4, 874–878, http://dx.doi.org/10.1038/NGEO1263.
Jackson, E.D., Shaw, H.R., 1975. Stress fields in central portions of the Pacific plate: delineated in time by linear volcanic chains. J. Geophys. Res. 80, 1861–1874, http://dx.doi.org/10.1029/JB080i014p01861.
Kerr, R.C., Mériaux, C., 2004. Structure and dynamics of sheared mantle plumes. Geochem. Geophys. Geosyst. 5, http://dxdoi.org/10.1029/2004GC000749.
Payne, J.A., Jackson, M.G., Hall, P.S., 2012. En echelon volcanism and geochemical asymmetry at the Societies hotspot. Geology, in press.
Ren, Z.-Y., et al., 2006. Isotope compositions of submarine Hana Ridge Lavas, Haleakala Volcano, Hawaii: implications for source compositions, melting process and the structure of the Hawaiian Plume. J. Petrol. 47, 255–275.
Ren, Z.-Y., Takeshi, H., Miyazaki, T., Chang, et al., 2009. Geochemical differences of the Hawaiian shield lavas: implications for melting processes in the heterogeneous Hawaiian plume. J. Petrol. 50, 1553–1573.
Ritsema, J., Deuss, A., van Heist, H.J., Woodhouse, J.H., 2011. S40RTS: a degree-40 shear velocity model for the mantle from new Rayleigh wave dispersion, teleseismic traveltime and normal-mode splitting function measurements. Geophys. J. Int. 184, 1223–1236.
Rohde, J., Hoernle, K., Hauff, F., Werner, R., O'Connor, J., Class, C., Garbe-Schnberg, D., Jokat, W., 2012. 80 Ma chemical zonation of the Tristan-Gough plume, Geology, in press.
Romanowicz, B., Gung, Y., 2002. Superplumes from the core-mantle boundary to the lithosphere: implications for heat flux. Science 296, 513–516.
Schmerr, N., Garnero, E., 2006. Investigation of upper mantle discontinuity structure beneath the central Pacific using SS precursors. J. Geophys. Res. 111, http://dx.doi.org/10.1029/2005JB004197.
Schmerr, N., Garnero, E., McNamara, A., 2010. Deep mantle plumes and convective upwelling beneath the Pacific Ocean. Earth Planet. Sci. Lett. 294, 143–151.
Steinberger, B., Sutherland, R., O'Connell, R.J., 2004. Prediction of Emperor-Hawaii seamount locations from a revised model of global plate motion and mantle flow. Nature 430, 167–173.
Steinberger, B., Torsvik, T.H., 2012. A geodynamic model of plumes from the margins of large low shear velocity provinces. Geochem. Geophys. Geosyst. 13, http://dx.doi.org/10.1029/2011GC003808.
Tackley, P.J., 1998. Three-dimensional simulations of mantle convection with a thermo-chemical basal boundary layer: D"? In: Gurnis, M. (Ed.), The Core-mantle boundary region, Geophys. Monogr. Ser., vol. 28. AGU, pp. 231–253.
Tanaka, R., Nakamura, E., 2005. Boron isotopic constraints on the source of Hawaiian shield lavas. Geochim. Cosmochim. Acta 69, 3385–3399.
Tanaka, R., Makishima, A., Nakamura, E., 2008. Hawaiian double volcanic chain triggered by an episodic involvement of recycled material: constraints from temporal Sr–Nd–Hf–Pb isotopic trend of the Loa-type volcanoes. Earth Planet. Sci. Lett. 265, 450–465.
Tosi, N., Yuen, D.A., 2011. Bent-shaped plumes and horizontal channel flow beneath the 660 km discontinuity. Earth Planet. Sci. Lett. 312, 348–359.
Weis, D., Garcia, M.O., Rhodes, J.M., Jellinek, M., Scoates, J.S., 2011. Role of the deep mantle in generating the compositional asymmetry compositional asymmetry of the Hawaiian mantle plume. Nat. Geosci. 4, 831–838, http://dx.doi.org/10.1038/NGEO1328.
Wen, L., 2006. A compositional anomaly at the Earth's core-mantle boundary as an anchor to the relatively slowly moving surface hotspots and as source to the DUPAL anomaly. Earth Planet. Sci. Lett. 246, 138–148.
Wessel, P., Kroenke, L., 1997. A geometric technique for relocating hotspots and refining absolute plate motions. Nature 387, 365–369.
West, H.B., Leeman, W.P., 1987. Isotopic evolution of lavas from Haleakala Crater, Hawaii. Earth Planet. Sci. Lett. 84, 211–225.
Wolfe, C.J., Solomon, S.C., Laske, G., Collins, J.A., Detrick, R.S., Orcutt, J.A., Bercovici, D., Hauri, E.H., 2009. Mantle shear-wave velocity structure beneath the Hawaiian hotspot. Science 326, 1388–1390.
Wolfe, C.J., Solomon, S.C., Laske, G., Collins, J.A., Detrick, R.S., Orcutt, J.A., Bercovici, D., 2011. Mantle P-wave velocity structure beneath the Hawaiian hotspot. Earth Planet. Sci. Lett. 303, 267–280.
Xu, G., et al., 2005. East Molokai and other Kea-trend volcanoes: magmatic processes and sources as they migrate away from the Hawaiian hot spot. Geochem. Geophys. Geosyst. 6, http://dx.doi.org/10.1029/2004GC000830.
Xu, G., Frey, F.A., Clague, D.A., Abouchami, W., Blichert-Toft, J., Cousens, B., Weisler, M., 2007. Geochemical characteristics of West Molokai shield- and postshield-stage lavas: constraints on Hawaiian plume models. Geochem. Geophs. Geosyst. 8, http://dx.doi.org/10.1029/2006GC001554.
Yamasaki, S., Kani, T., Hanan, B.B., Tagami, T., 2009. Isotopic geochemistry of Hualalai shield-stage tholeitic basalts from submarine North Kona region, Hawaii. J. Volcanol. Geotherm. Res. 185, 223–230.
Yu, Y.G., Wentzcovitch, R.M., Vinograd, V.L., Angel, R.J., 2011. Thermodynamic properties of $MgSiO_3$ majorite and phase transitions near 660 km depth in $MgSiO_3$ and Mg_2SiO_4: a first principles study. J. Geophys. Res. 116, http://dx.doi.org/10.1029/2010JB007912.